

# Studies on Phase Separation Rate in Porous Polyimide Membrane Formation by Immersion Precipitation

Hideto Matsuyama, Keizo Nakagawa, Taisuke Maki, Masaaki Teramoto

Department of Chemistry and Materials Technology, Kyoto Institute of Technology, Matsugasaki, Sakyo-ku, Kyoto 606-8585, Japan

Received 29 May 2002; accepted 14 January 2003

**ABSTRACT:** Phase separation rate during porous membrane formation by immersion precipitation was investigated by light scattering in a polyimide/N-Methylpyrrolidone (NMP)/water system. In the light scattering measurement, plots of scattered intensity against scattered angle showed maxima in all cases, which indicated that phase separation occurred by a spinodal decomposition (SD). Characteristic properties of the early stage of SD, such as an apparent diffusion coefficient  $D_{app}$  and an interphase periodic distance  $\Lambda$ , were obtained. The growth process of  $\Lambda$  was

also followed by light scattering. The growth rate had the same tendency as  $D_{app}$  when water content in the nonsolvent bath and the polymer concentration in the cast solution were changed. The pore size of the final membrane increased with decreasing water content, which was opposite to the tendency of  $\Lambda$  growth rate. © 2003 Wiley Periodicals, Inc. *J Appl Polym Sci* 90: 292–296, 2003

**Key words:** microporous polyimide membrane; phase separation; light scattering

## INTRODUCTION

The immersion precipitation method is one of the major phase separation methods to produce a porous polymeric membrane.<sup>1</sup> A polymer solution is cast on a support and is subsequently immersed in a nonsolvent coagulation bath. Phase separation occurs because of the inflow of nonsolvent to the cast solution.

To understand and control the membrane structure, two factors, equilibrium phase diagram and kinetics, must be clarified. The equilibrium phase diagram can show the stable region of the cast solution and types of phase separation such as nucleation and growth (NG) and spinodal decomposition (SD). The phase diagram for a three-component system of polymer, solvent, and nonsolvent was analyzed based on the Flory-Huggins theory.<sup>2–5</sup>

Two kinds of kinetics play an important role in a porous membrane formation by the immersion precipitation method; that is, a change of composition due to the exchange of solvent and nonsolvent, and phase separation rate. Many mass transfer models have been developed to calculate the change of composition during membrane formation.<sup>6–9</sup> The ultimate membrane structure can be predicted to some extent by the calculated composition change path. Although most of the models were useful only before the phase separation, Kim et al. recently extended the calcula-

tion to include post-phase separation.<sup>10</sup> Several studies have been presented in measuring phase separation rate mainly in the initial early stage of the phase separation by the light scattering method.<sup>11–14</sup> Nunes and Inoue found the conditions for SD or NG based on the light scattering profiles.<sup>11</sup>

Very few studies have been reported on the structure growth rate in the latter stage of the phase separation of the porous membrane formation process. However, knowledge of this growth rate is important because the ultimate structure is directly related to this process. We measured the structure growth rate in the dry-cast process and studied the effects of experimental conditions on the growth rate.<sup>15</sup> In the dry-cast process, the evaporation of the solvent leads to a decrease of the polymer solubility and then phase separation can take place. The solvent evaporation rate in the dry-cast process is generally slower than the exchange rate between solvent and nonsolvent in the immersion precipitation process. Thus, the light scattering measurement can be carried out more easily in the dry-cast process.

In this work, the membrane formation by the immersion precipitation was studied by the light scattering method. The structure growth rate was measured, as well as the initial phase separation rate under several conditions. This fundamental study is believed to be important for application to membrane preparation.

## EXPERIMENTAL

### Materials

Polymer was poly [N,N'-(1,4-phenylene)-3,3',4,4'-benzophenonetetracarboxylic imide/amic acid] (BTDA-p-

Correspondence to: H. Matsuyama (matuyama@chem.kit.ac.jp).

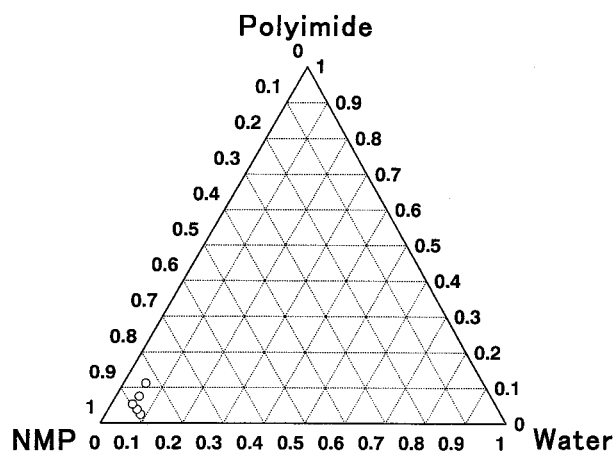


**Figure 1** Phase diagram in polyimide/NMP/water system. ○: cloud point, Volume fractions were used in this figure.

PDA imide, Aldrich Chemical Inc.,  $M_w = 89000$ ,  $M_n = 43000$ ). N-Methylpyrrolidone (NMP, Wako Pure Chemical Industries Ltd., Osaka, Japan) was used as solvent and nonsolvent was water.

### Cloud point

Homogeneous polymer solutions of 3, 5, 7, 10, and 15 wt % polymer concentration were prepared at 25°C. A small amount of nonsolvent was then successively added to the solution. Cloud point was determined visually by noting the appearance of turbidity.

### Lights scattering experiment

The light scattering measurement was carried out with a polymer dynamics analyzer (Otsuka Electronics Co., DYNA-3000, Hirakata, Japan). The polymer solution was cast on the glass plate with thickness of 254  $\mu\text{m}$ . The cast solution with the glass plate was immersed in the nonsolvent bath located between the laser and the detector. The nonsolvent solutions were mixtures of water and NMP with several ratios. The temperature of the nonsolvent was about 25°C. The light scattering, due to phase separation after immersion in the bath, was followed at time intervals of 0.22 s.

### Membrane morphology

The cast membrane was kept immersed in the nonsolvent bath for 1 day, and then the membrane was dried at room temperature. For scanning electron microscope (SEM) observation, the membrane was immersed in liquid nitrogen, fractured, and coated with Au/Pd. The cross section was viewed by a scanning electron microscope (Hitachi Co. Ltd., Japan, S-800) under an accelerating voltage of 15 kV.

## RESULTS AND DISCUSSION

Figure 1 shows the phase diagram in polyimide/NMP/water system. Cloud points are plotted as circles. Even the addition of a small amount of water brings about phase separation in this system. For example, when the polymer volume fraction is 0.11, water volume fraction necessary for the phase separation is about 0.05.

Figure 2(a) shows an example of the light scattering experiment in a short time interval. The scattered intensity  $I_s$  shows a maximum, which indicates that the phase separation occurred by SD rather than by NG.<sup>10</sup> The location of the maximum of  $I_s$  was constant in this time scale. This means that the size of the structure, derived from the phase separation, is unchanged. This stage corresponds to the early stage of SD. The result of the same system over a longer time interval is shown in Figure 2(b). The position of  $I_s$  peak shifted to the smaller angle region with time, accompanying an increase of intensity. This shift of the peak position into the smaller angle region indicates the growth of the structure. The phase separation in this time scale is at an intermediate or late stage of SD.

In the early stage of SD, growth rate of the concentration fluctuation  $R(q)$  can be related to a wavenumber  $q$  as Eq. (1) based on the linear Cahn theory.<sup>16,17</sup>

$$R(q)/q^2 = D_{\text{app}}(1 - q^2/2q_m^2) \quad (1)$$

Here,  $q$  is given by Eq. (2) and  $D_{\text{app}}$  and  $q_m$  are the apparent diffusion coefficient and the wavenumber of maximum  $I_s$ , respectively.

$$q = 4\pi n_0/\lambda_0 \sin(\theta/2) \quad (2)$$

$n_0$  is the reflection coefficient and  $\lambda_0$  is the wavelength in vacuo (633 nm). Examples of plots of  $R(q)/q^2$  against  $q^2$  are shown in Figure 3. Linear relations were obtained, which is in accordance with the theoretical expectation expressed by Eq. (1). The intercepts of the straight lines give  $D_{\text{app}}$ . The values of  $D_{\text{app}}$  in several

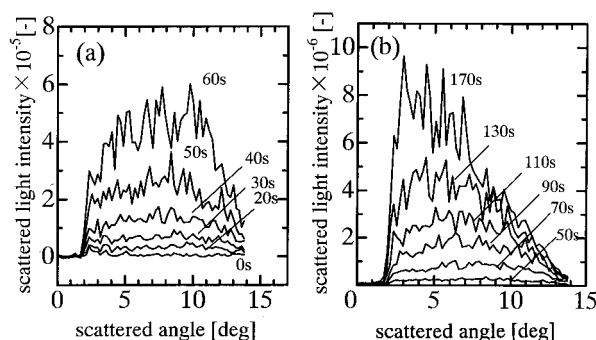


**Figure 2** Light scattering profiles. Polymer concentration = 15 wt %, ratio of water to NMP in nonsolvent bath = 8:92. (a) shorter time period, (b) longer time period.

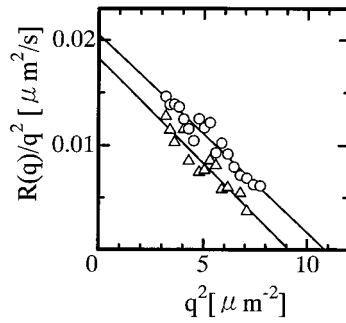


**Figure 3** Relation between  $R(q)/q^2$  and  $q^2$ . Ratio of water to NMP in nonsolvent bath = 8:92. ○: polymer concentration = 10 wt %, △: polymer concentration = 15 wt %.

cases are summarized in Table I, together with the interphase periodic distance  $\Lambda$  in the early stage of SD, which is given by Eq. (3)

$$\Lambda = \frac{\lambda_0}{2n_0 \sin(\theta/2)} \quad (3)$$

When the composition of the nonsolvent bath solution is the same,  $D_{app}$  decreased with the increase of polymer concentration in the cast solution.  $D_{app}$  depends on both thermodynamic and kinetic aspects.<sup>11</sup>  $D_{app}$  is higher when the self-diffusion coefficient of polymer is higher and the quench depth (distance from the spinodal line) is deeper. The self-diffusion coefficient is lower in the cast solution with the higher polymer concentration, due to the higher solution viscosity. In addition, the high polymer concentration leads to a shallow quench depth because the higher solution viscosity depresses the water inflow into the cast solution. Due to these two reasons,  $D_{app}$  was lower in the high polymer concentration.  $\Lambda$  is related to the quench depth, that is, deeper quench depth gives the smaller  $\Lambda$ .<sup>18</sup> As shown in Table I,  $\Lambda$  increases with the increase of the polymer concentration because of the shallow quench. When the polymer concentration is the same, the higher  $D_{app}$  and the lower  $\Lambda$  are obtained as the water content in the nonsolvent bath solution increases. The higher water content leads to the high rate of the water inflow, which results in the deeper quench depth. The behavior of  $D_{app}$  and  $\Lambda$  can be explained by this relationship with quench depth.

**TABLE I**  
 **$D_{app}$  and Interphase Periodic Distance  $\Lambda$**

Ratio of water to NMP in nonsolvent bath	Polymer concentration (wt %)	$D_{app} \times 10^2$ [ $\mu\text{m}^2/\text{s}$ ]	$\Lambda$ [ $\mu\text{m}$ ]
8:92	10	2.05	2.69
8:92	15	1.83	2.98
8:92	20	0.59	3.17
10:90	10	2.21	2.31

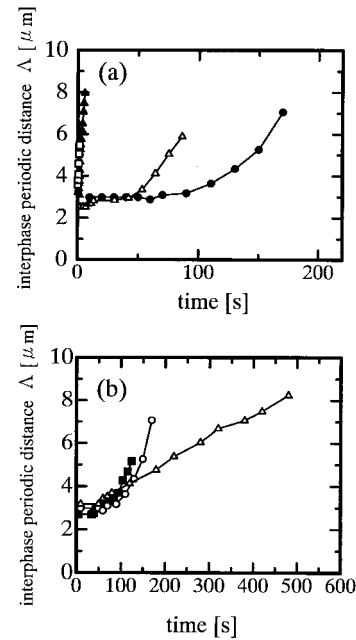


**Figure 4** Time courses of the interphase periodic distance  $\Lambda$ . (a) Effect of nonsolvent bath composition. Polymer concentration = 15 wt %. ●: ratio of water to NMP in nonsolvent bath = 8:92, △: 10:90, ▲: 13:87, □: 15:85. (b) Effect of polymer concentration. Ratio of water to NMP in nonsolvent bath = 8:92. ■: polymer concentration = 10 wt %, ○: 15 wt %, △: 20 wt %.

Figure 4(a) shows the time course of  $\Lambda$  when the water content in the nonsolvent bath solution was changed. In the cases of water contents of 8 and 10 wt %,  $\Lambda$  was initially constant and then increased. The period for the constant  $\Lambda$  corresponds to the early stage of SD. When the water contents were 13 and 15 wt %, the growth rate was too fast for the early stage of SD to be recognized. As the water content increased, the structure growth rate clearly increased. It has been reported that the structure growth rate increases with increasing quench depth<sup>19,20</sup> and the period for the early stage of SD becomes shorter.<sup>21</sup> As described above, the quench depth becomes deeper with the increase of the water content. Thus, the growth rate increases and the period in the early stage decreases as the water content increases.

Figure 4(b) shows the effect of the polymer concentration on the growth rate. Although  $\Lambda$  at the early stage of SD increases with increasing the polymer concentration, as shown in Table I, the growth rate shows the opposite tendency, that is; it decreases at the high polymer concentration. Thus, the order of magnitude of  $\Lambda$  is contrary to that in the early stage. The decrease of the growth rate is attributable to the shallower depth and the higher solution viscosity.

Figure 5 shows the cross sections of the membranes when the water content in the nonsolvent bath was changed. As the water content decreased, the forma-

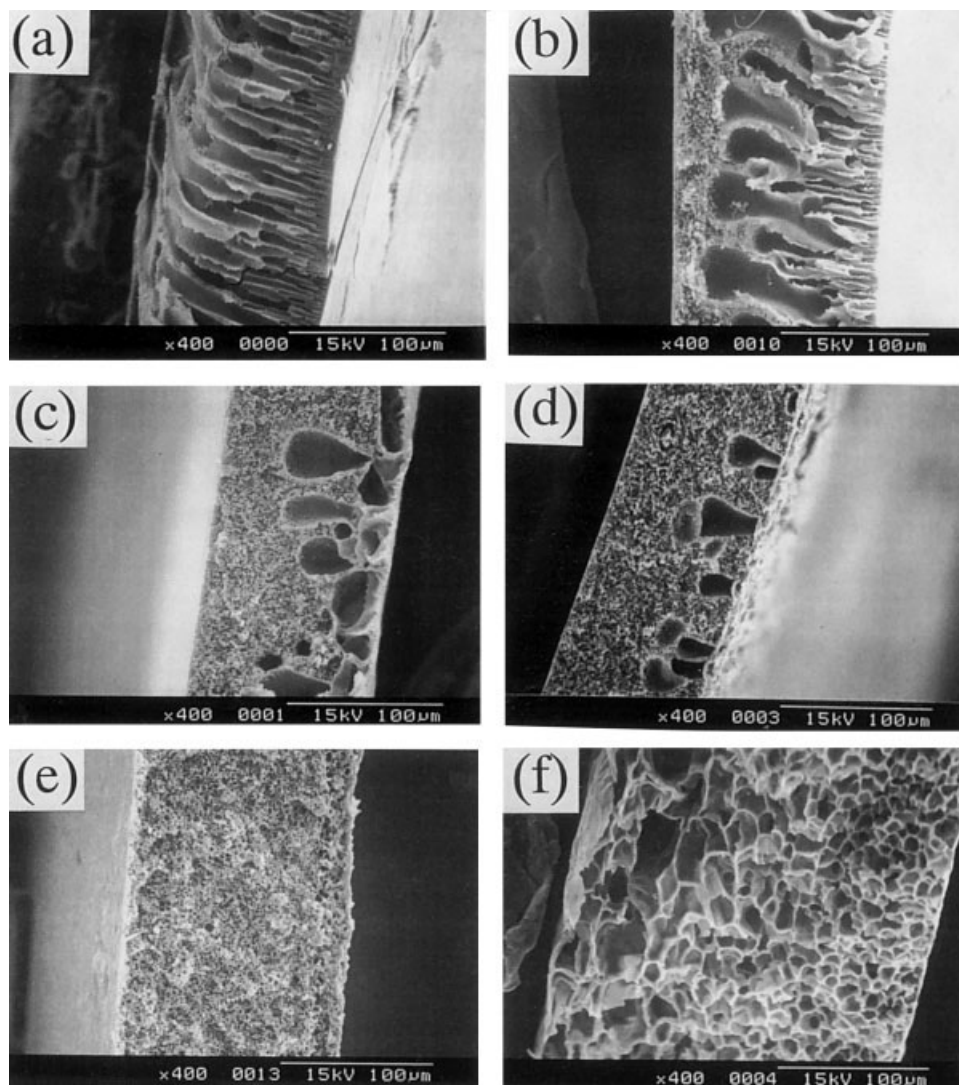


**Figure 5** Cross sections of porous membranes prepared when water content in the nonsolvent bath was changed. (a) water:NMP= 100:0, (b) 20:80, (c) 15:85, (d) 13:87, (e) 10:90, (f) 8:92. Right and left sides correspond to top and glass surfaces, respectively.

tion of a macrovoid (large cavity of a conical shape) was prevented. It has been recognized that the delayed demixing of the cast solution during the membrane formation has a tendency to prevent macrovoid formation.<sup>22,23</sup> The addition of solvent to the nonsolvent bath promoted the delayed demixing, which resulted in the suppression of the macrovoid formation.

Figure 6 shows the membrane structures near the top surface at a higher magnification. The pore sizes increased with the decrease of the water content. As shown in Figure 4(a), the structure growth rate, measured by the light scattering method, decreased in this order. Thus, the tendency of the pore size in the porous membrane was opposite to that of the structure growth rate. The pore can grow until the matrix phase (polymer rich phase) is solidified by the glass transition or gelation. When the water content is lower, the quench depth is shallower, which means that the poly-

mer concentration of the polymer rich phase is lower. Therefore, there is a longer time until membrane solidification. If this factor of the growth time is more pronounced than that of the growth rate, the ultimate pore size can become larger in the lower water content condition.

## CONCLUSION

The phase separation rate in porous polyimide membrane formation by the immersion precipitation was studied by a light scattering method. In the light scattering measurement, the scattered intensity  $I_s$  showed maxima in all cases, which indicated that the phase separation occurred by SD.

The early stage of SD was studied. The apparent diffusion coefficient  $D_{app}$  and the interphase periodic distance  $\Lambda$  were obtained under several experimental

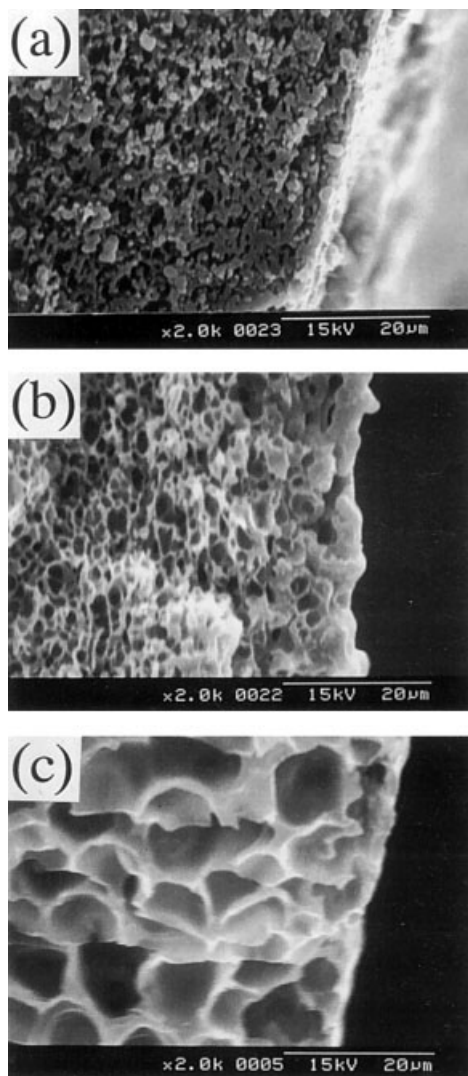


**Figure 6** Membrane structures near top surfaces. (a) water:NMP = 13:87, (b) 10:90, (c) 8:92.

conditions.  $D_{app}$  increased and  $\Lambda$  decreased as the water content in the nonsolvent bath increased and the polymer concentration in the cast solution decreased. The quench depth and the solution viscosity varied accordingly.

The growth rate of  $\Lambda$  was measured from the shift of maximum  $I_s$  position. The growth rate had the same

tendency as  $D_{app}$  when the water content and the polymer concentration were changed.

The membrane cross sections were observed. The macrovoid formation was suppressed by the addition of solvent to the nonsolvent bath. The pore size increased with decreasing the water content. This was opposite to the behavior of the growth rate of  $\Lambda$ .

## References

1. van de Witte, P.; Dijkstra, P. J.; van den Berg, J. W. A.; Feijen, J. *J Membrane Sci* 1996, 117, 1.
2. Flory, P. J. *Principles of polymer chemistry*, Cornell University Press, Ithaca, NY, 1953
3. Altena, F. W.; Smolders, C. A. *Macromolecules* 1982, 15, 1491.
4. Yilmaz, L.; McHugh, A. J. *J Appl Polym Sci* 1986, 31, 997.
5. Cheng, L. P.; Dwan, A. H.; Gryte, C. C. *J Polym Sci B Polym Phys* 1994, 32, 1183.
6. Reuvers, A. J.; van den Berg, J. W. A.; Smolders, C. A. *J Membrane Sci* 1987, 34, 45.
7. Tsay, C. S.; McHugh, A. J. *J Polym Sci B Polym Phys* 1990, 28, 1327.
8. Radovanovic, P.; Thiel, S. W.; Hwang, S. T. *J Membrane Sci* 1992, 65, 213.
9. Cheng, L. P.; Dwan, A. H.; Gryte, C. C. *J Polym Sci B Polym Phys* 1995, 33, 223.
10. Kim, Y. D.; Kim, J. Y.; Lee, H. K.; Kim, S. C. *J Membrane Sci* 2001, 190, 69.
11. Nunes, S. P.; Inoue, T. *J Membrane Sci* 1996, 111, 93.
12. Zoppi, R. A.; Contant, S.; Duek, E. A. R.; Marques, F. R.; Wada, M. L. F.; Nunes, S. P. *Polymer*, 40, 3275.
13. Barth, C.; Gongalves, M. C.; Pires, A. T. N.; Roeder, J.; Wolf, B. A. *J Membrane Sci* 2000, 169, 287.
14. Schuhmacher, E.; Soldi, V.; Pires, A. T. N. *J Membrane Sci* 2001, 184, 187.
15. Matsuyama, H.; Tachibana, M.; Maki, T.; Teramoto, M. *J Appl Polym Sci*, submitted
16. Hashimoto, T.; Kumaki, J.; Kawai, H. *Macromolecules* 1983, 16, 641.
17. Lal, J.; Bansil, R. *Macromolecules* 1991, 24, 290.
18. Sasaki, K.; Hashimoto, T. *Macromolecules* 1984, 17, 2818.
19. Graham, P. D.; McHugh, A. J. *Macromolecules* 1998, 31, 2565.
20. Song, S. W.; Torkelson, J. M. *Macromolecules* 1994, 27, 6389.
21. Maki, T.; Matsuyama, H.; Teramoto, M. *Kagaku Kogaku Ronbunshu*, 2001, 27, 742
22. Mulder, M. *Basic Principles of Membrane Technology*; Kluwer Academic Publishers: Dordrecht, 1996.
23. Zeman, L. J.; Zydney, A. L. *Microfiltration and Ultrafiltration*; Marcel Dekker Inc.: New York, 1996.